Exosomal miR-136-5p Derived From Anlotinib-Resistant NSCLC Cells Confers Anlotinib Resistance in Non-Small Cell Lung Cancer Through Targeting PPP2R2A

Guoqing Gu
The Affiliated Lianyungang Hospital of Xuzhou Medical University
Chenxi Hu
The Affiliated Lianyungang Hospital of Xuzhou Medical University
Kaiyuan Hui
The Affiliated Lianyungang Hospital of Xuzhou Medical University
Huiqin Zhang
The Affiliated Liayungang Hospital of Xuzhou Medical University
Ting Chen
The Affiliated Lianyungang Hospital of Xuzhou Medical University
Xin Zhang
Lianyungang Clinical College of Nanjing Medical University
Xiaodong Jiang (jiangxiaodong_jxd@126.com)
The Affiliated Lianyungang Hospital of Xuzhou Medical University

Research

Keywords: Advanced non-small cell lung cancer, anlotinib resistance, exosome, microRNA

Posted Date: June 7th, 2021

DOI: https://doi.org/10.21203/rs.3.rs-541122/v1

Abstract

Background: Anlotinib resistance is a challenge for advanced non-small cell lung cancer (NSCLC). Understanding the underlying mechanisms against anlotinib resistance is of great importance to improve prognosis and treatment of patients with advanced NSCLC.

Methods: RT-qPCR assay was used to assess the level of miR-136-5p in anlotinib-resistant NSCLC cells and exosomes derived from anlotinib-resistant NSCLC cells. CCK-8 assay was performed to assess cell viability.

Results: High levels of plasma exosomal miR-136-5p is correlated with clinically poor anlotinib response. In addition, anlotinib-resistant NSCLC cells promoted parental NSCLC cell proliferation via transferring functional miR-136-5p from anlotinib-resistant NSCLC cells to parental NSCLC cells via exosomes. Moreover, exosomal miR-136-5p could endow NSCLC cells with anlotinib resistance by targeting PPP2R2A, leading to the activation of Akt pathway. Furthermore, miR-136-5p antagomir packaging into anlotinib-resistant NSCLC cell-derived exosomes functionally restored NSCLC cell anlotinib sensitivity.

Conclusion: Collectively, these findings indicated that anlotinib-resistant NSCLC cell-derived exosomal miR-136-5p confers anlotinib resistance in NSCLC cells by targeting PPP2R2A, indicating miR-136-5p may act as a potential biomarker for anlotinib response in NSCLC.

Introduction

Non-small cell lung cancer (NSCLC) is the most common type of lung cancer (1, 2). In addition, NSCLS is characterized by highly invasive behavior, resistance to chemotherapy and poor prognosis (3, 4). Despite advances in diagnosis and treatment strategies, the prognosis of NSCLC patients remain unsatisfactory (5, 6). Therefore, deeper investigation into the exploration of novel therapies of NSCLC are particularly important. Anlotinib is an orally administered multikinase inhibitor, which has inhibitory effects on tumor growth and angiogenesis due to the inhibition of vascular endothelial growth factor receptor (VEGFR) 1 to 3, stem cell factor receptor (c-kit), platelet-derived growth factor receptors and fibroblast growth factor receptor 1 to 4 (6). In addition, anlotinib are currently available as third-line regimen for advanced NSCLC patients (7). Significantly, anlotinib could prolong progression-free survival and overall survival in patients with NSCLC (7). However, drug resistance in NSCLC is inevitable. Therefore, it is urgent to investigate the underlying mechanisms of anlotinib resistance in patients with NSCLC and explore novel biomarkers to predict sunitinib response.

Exosomes (50–150 nm) are nanosized that are actively released by a variety of cells and are released into the extracellular milieu (8, 9). In addition, exosomes have been found to be participating in cell-to-cell communication by transmitting many bioactive molecules, such as proteins, lipids, microRNAs (miRNAs) (10, 11). Evidence has shown that tumor cell-derived exosomes play an important role in the development of cancer malignancy via regulating drug resistance (12). However, whether tumor cell-derived exosomes could confer drug resistance in sensitive cells has not been fully investigated.

MiRNAs are a group of noncoding RNA molecules that post-transcriptionally regulate gene expression by interaction with the 3'-UTRs of target mRNAs (13, 14). In addition, miRNAs have shown to play pivotal roles in several biological processes, such cell proliferation, metastasis and apoptosis (15). Meanwhile, it has been shown that miRNAs participated in mediating the resistance in human cancers (16). However, the roles of miRNAs in anlotinib resistance in NSCLC are poorly illuminated. Thus, in this study, we aimed to investigate the role of exosomal miRNAs in the regulation of anlotinib resistance of NSCLC.

Materials And Methods

Patient samples

All clinical samples were collected from patients with NSCLC from the Affiliated Lianyungang Hospital of Xuzhou Medical University, and written informed consent was obtained from all patients. In addition, the ethical approval was approved by the ethics committee of the Affiliated Lianyungang Hospital of Xuzhou Medical University.

RNA sequencing

Exosomes were isolated from plasma samples using the GETTM Exosome Isolation Kit (GeneExosome technologies). After that, total RNA was extracted from exosomes using miRNeasy® Mini kit (Qiagen) according to the manufacturer's protocol. Sequencing libraries were prepared from all samples using QIAseq miRNA Library Kit. After that, the libraries were quantified by Agilent Bioanalyzer 2100 and sequenced by Illumina Hiseq sequencer (Illumina, San Diego, CA, USA). The prepared sequences were then filtered and aligned using Bowtie tool against the human miRNA sequences downloaded from miRbase.

Function enrichment analyses

The target genes of differentially expressed miRNAs (DEMs) were subjected to Gene Ontology (GO) enrichment and Kyoto Encyclopedia of Genes and Genomes (KEGG) pathway analyses using the online tool KOBAS (17).

Cell culture and cell transfection

Human NSCLC cell lines A549 and NCI-H1975 were purchased from American Type Culture Collection. Two anlotinib-resistant NSCLC cell lines (A549/ anlotinib and NCI-H1975/anlotinib) were generated from parental A549 and NCI-H1975 cells by gradually treating them with increasing doses of anlotinib for more than 3 months. A549, NCI-H1975, A549/anlotinib and NCI-H1975/anlotinib cell lines were cultured in DMEM medium supplemented with 10% FBS, 100 μ/mL penicillin and 0.1 mg/mL streptomycin and maintained in a humidified incubator containing 5% CO_2 at 37°C.

Cells were transfected with miR-136-5p agomir, miR-136-5p antagomir and PPP2R2A siRNA1 or PPP2R2A siRNA2 (Ribobio, Guangzhou, China) using Lipofectamine 2000 transfection reagent according to the

manufacturer's protocols.

Cell Counting Kit-8 (CCK-8) assay

Cell viability was monitored using a CCK-8 assay kit (Dojindo, Kumamoto, Japan). Cells were seeded onto 96-well culture plates at 5×10^3 cells/well, and then treated with CCK-8 reagent (10 μL per well). Subsequently, the absorbance was measured by measuring the absorbance at 450 nm in a microplate reader.

Exosome isolation and characterization

Exosomes secreted by A549 and A549/anlotinib cells were isolated by using the GETTM Exosome Isolation Kit (GeneExosome technologies). The exosome samples were detected on a ZetaView Nanoparticle tracking analysis (NTA) instrument. In addition, exosomes were identified by transmission electron microscopy (TEM) and confirmed by the expression of exosome markers TSG101 and CD81.

Exosome uptake

A549 and A549/anlotinib cell-derived exosomes were labeled with PKH26 dye for 30 min at 37°C to observe the uptake of exosomes in A549 cells. Subsequently, the internalization of exosomes was measured by a confocal microscope. Nuclei were stained by DAPI.

Co-culture system

Cy3-labeled miR-136-5p was transfected into A549/anlotinib cells. After that, the transfected A549/anlotinib cells were seeded on a Transwell® polyester permeable supports. In addition, A549 cells were plated on the lower chamber. After 24 h of incubation, cells were imaged using a fluorescence microscope (Olympus).

Flow cytometry assay

For the cell apoptosis assay, cells were collected and washed twice with cold PBS. After that, cells were incubated with 10 μL of Annexin V-FITC and propidium iodide (PI) for 30 min in darkness. Subsequently, apoptotic cells were assessed by a flow cytometer (BD Biosciences).

For the cell cycle assay, cells were collected and fixed in 70% ethanol for 30 min. After that, cells were treated with RNase A for 20 min at 37°C and then stained for 30 min in darkness with 1 mg/mL PI. Subsequently, cell cycle distribution was assessed using a flow cytometer.

Western blot assay

Total protein from NSCLC cells were quantified by the Pierce BCA Protein assay kit. After that, proteins were subjected to 10% SDS-PAGE and then transferred onto PVDF membranes. After blocking with 5% non-fat milk for 1 h, membranes were incubated with primary antibodies against p-Akt, Akt, p-ERK, ERK,

BCL-2, XIAP, PPP2R2A, β-actin at 4°C overnight. Later on, membranes were incubated with the corresponding HRP-labeled goat anti-rabbit secondary antibodies at room temperature for 1 h. Subsequently, protein bands were visualized using a chemiluminescence detection kit (Thermo Fisher Scientific). All antibodies were procured from Abcam (Cambridge, MA).

RT-qPCR assay

Total RNA was isolated from cells using the TRIpure Total RNA Extraction Reagent. Later on, total RNA was reversely transcribed using EntiLink™ 1st Strand cDNA Synthesis Kit (ELK Biotechnology). After that, real-time PCR was run with StepOne™ Real-Time PCR System and EnTurbo™ SYBR Green PCR SuperMix kit (ELK Biotechnology). U6 was used as an internal reference of miR-136-5p. Fold changes were calculated by using the $2^{-\Delta\Delta CT}$ formula. U6: 5'- CTCGCTTCGGCAGCACAT-3' (F); 5'-AACGCTTCACGAATTTGCGT-3' (R). miR-136-5p: 5'-TCCATTTGTTTTGATGATGGACT-3' (F); 5'-CTCAACTGGTGTCGTGGAGTC-3' (R).

EdU staining assay

Cell proliferation was measured by an EdU kit (Cell-Light EdU Apollo567 In Vitro Kit; Ribobio). Cells were incubated with EdU for 2 h, fixed in 4% paraformaldehyde and permeated with 0.3% TritonX-100 for 15 min. Later on, cells were stained with apollo dye, and then incubated with Hoechst33342 for 30 min. Subsequently, EdU-positive cells was captured using a fluorescence microscope.

Dual-luciferase reporter assay

The wild-type (WT) and mutated (MT) miR-136-5p target in the PPP2R2A 3'-UTR were cloned into the pGL6-miR-based luciferase reporter plasmids. Later on, the above recombinant plasmids were co-transfected with miR-136-5p agomir or its negative control using Lipofectamine 2000 for 48 h. Subsequently, luciferase activity was monitored using the Dual-Luciferase Reporter Assay System (Promega Madison, WI) with renilla luciferase activity as endogenous control.

Animal study

BALB/c nude mice (4-week-old and 16–20 g in weight) were purchased from the Experimental Animal Center of Soochow University. A549 cells (10^7 cells) were subcutaneously injected into left flank of nude mice. When the tumors reach about 200 mm^3, animals were divided randomly into 5 groups: control, PBS + anlotinib treatment, (NSCLC-anlotinib-NC)-Exo + anlotinib treatment, (NSCLC-anlotinib-miR-136-5p agomir)-Exo + anlotinib treatment, or (NSCLC-anlotinib-miR-136-5p antagomir)-Exo + anlotinib treatment groups. After that, PBS, (NSCLC-anlotinib-NC)-Exo, (NSCLC-anlotinib-miR-136-5p agomir)-Exo, or (NSCLC-anlotinib-miR-136-5p antagomir)-Exo was directly injected into the tumors twice a week for 3 weeks. In addition, mice were administered anlotinib (4 mg/kg) by oral gavage for 2 weeks. Tumor volume was calculated every week using the following formula: volume = 0.5 x length × $width^2$. Later on, the mice were euthanized at day 21, and the tumors were removed and weighted. The APO-BrdU™ TUNEL Assay Kit

was used to evaluate cell apoptosis in tumor tissues. Animal study was approved by the ethics committee of the Affiliated Lianyungang Hospital of Xuzhou Medical University.

Statistical analysis

Results were all exhibited as the mean ± standard deviation (S.D.). Differences between three or more groups were analyzed by One-way analysis of variance (ANOVA) and Tukey's tests using GraphPad Prism software (version 7.0). Differences between two groups were analyzed by two-tailed Student's t-test. The difference was significant with a value of *P < 0.05. All data were repeated in triplicate.

Results

NSCLC/anlotinib cell-derived exosomes increased NSCLC cell proliferation and anlotinib resistance

To compare the viability between the anlotinib-sensitive and anlotinib-resistant NSCLC cells, A549, A549/anlotinib cells, and NCI-H1975, NCI-H1975/anlotinib cells were grown in medium containing with different concentrations of anlotinib for 72 h. As indicated in Figure 1A and 1B, anlotinib reduced the viability of A549, A549/anlotinib cells, and NCI-H1975, NCI-H1975/anlotinib cells in a dose-dependent manner. In addition, 20 μM anlotinib induced about 74% and 76% growth inhibition of A549 and NCI-H1975 cells respectively, whereas 20 μM anlotinib induced about 15% and 10% growth inhibition of A549/anlotinib and NCI-H1975/anlotinib cells (Figure 1A and 1B). These data suggested that A549/anlotinib and NCI-H1975/anlotinib cells were resistant to anlotinib.

Next, we investigated whether functional factors secreted by anlotinib-resistant NSCLC cells could affect the viability of anlotinib-sensitive NSCLC cells. First, A549 and NCI-H1975 cells were cultured in the CM from A549/anlotinib (A549/anlotinib-CM) and NCI-H1975/anlotinib cells (NCI-H1975/anlotinib-CM) respectively. As indicated in Figure 1C, A549/anlotinib-CM and NCI-H1975/anlotinib-CM significantly promoted the viability of A549 and NCI-H1975 cells respectively. Additionally, cell viability rate was markedly increased in A549 and NCI-H1975 cells grown in A549/anlotinib-CM and NCI-H1975/anlotinib-CM and subsequently treated with anlotinib, compared with A549 and NCI-H1975 cells grown in A549-CM and NCI-H1975-CM respectively (Figure 1D). These data indicated that anlotinib-resistant NSCLC cells-CM that contained several functional factors could promote NSCLC cells proliferation and anlotinib resistance.

Exosomes are nanoparticles that play an important role in cell-to-cell communication (18). We have found that anlotinib-resistant NSCLC cells-CM could promote NSCLC cells proliferation and anlotinib resistance. Then, we investigated whether anlotinib-resistant NSCLC cell-derived exosomes contribute to this effect. Significantly, removing exosomes from A549/anlotinib-CM through ultracentrifugation or inhibiting the exosome secretion of A549/anlotinib-CM through GW4869 suppressed the ability of A549/anlotinib-CM to increase A549 cell viability and anlotinib resistance (Figure 2A). We then isolated exosomes from A549-CM (A549-Exo) and A549/anlotinib-CM (A549/anlotinib-Exo), and confirmed their identity by NTA, TEM and western blot assays. As shown in Figure 2B and 2C, A549-Exo and

A549/anlotinib-Exo are 50–150 nm diameter and exhibited typical cup-shaped structures. In addition, the specific surface markers in exosomes, such as TSG101 and CD81, were positively expressed in these vesicles (Figure 2D). Thus, A549-Exo and A549/anlotinib-Exo were isolated successfully.

To assess whether A549-Exo and A549/anlotinib-Exo could be internalized by A549 cells, we labeled A549-Exo and A549/anlotinib-Exo with PKH26 dye and added them into A549 cell culture medium. As revealed in Figure 2E, PKH26 dye was observed in A549 cells. Functionally, the results of CCK-8 and flow cytometry assays showed that A549 cells incubated directly with A549/anlotinib-Exo displayed reduced sensitivity to anlotinib (Figure 2F and 2G). Evidences have shown that Akt and ERK signaling pathways is usually associated with drug resistance of NSCLC cells (19, 20). As indicated in Figure 2H, A549/anlotinib-Exo endowed A549 cells with resistance to anlotinib and activated Akt and ERK signaling. Collectively, A549/anlotinib-Exo could confer anlotinib resistance to A549 cells.

MiR-136-5p is highly expressed in anlotinib-resistant NSCLC cells

In an attempt to explore the functional molecules required for the ability of A549/anlotinib-Exo to promote proliferation and anlotinib resistance in A549 cells, we purified exosomes from plasma samples in patients who exhibited a good response to anlotinib therapy and patients who exhibited a positive response to anlotinib initially and developed a resistance to anlotinib eventually (Table 1), and confirmed their identity by NTA, TEM and western blot assays (Figure 3A, 3B and 3C). Next, RNA-sequencing was performed to analyze the differentially expressed miRNAs (DEMs) in these isolated exosomes. As shown in Figure 3D and 3E, 14 upregulated miRNAs and 15 downregulated miRNAs were detected in exosomes derived from plasma samples in patients with poor anlotinib response relative to patients with good anlotinib response. To gain a more in-depth understanding of the DEMs, the target genes of DEMs were analyzed using GO enrichment and KEGG pathway analyses. GO results indicated that the target genes of DEMs were mainly enriched in the categories “cellular process”, “growth”, “molecular transducer activity” and “enzyme regulator activity” (Supplementary figure 1). As to KEGG pathway analysis, osteoclast differentiation, microRNAs in cancer, tight junction, transcriptional mis-regulation in cancer, were mostly associated with the target genes of DEMs (Supplementary figure 2).

Evidence has shown that miR-136-5p expression is associated with drug resistance in NSCLC (21). Significantly, miR-136-5p levels in tumor tissues and plasma were higher in patients who exhibited a poor response to anlotinib therapy compared with patients who were therapy naïve or patients who exhibited a positive response to anlotinib therapy (Figure 4A and 4B). Moreover, the level of miR-136-5p is upregulated in A549/anlotinib and NCI-H1975/anlotinib cells compared with that in their parental A549 and NCI-H1975 cells (Figure 4C). Meanwhile, the level of miR-136-5p was higher in the CM of anlotinib-resistant NSCLC cells than that in the CM of NSCLC cells (Figure 4D). Furthermore, high miR-136-5p levels were detected in the serum of mice xenografted with A549/anlotinib cells as well (Figure 4E). These data suggested that miR-136-5p was abundant in anlotinib-resistant NSCLC.

Exosomal transfer of miR-136-5p from anlotinib-resistant NSCLC cells to NSCLC cells

To investigate whether miR-136-6p could be transfer from A549/anlotinib cells to A549 cells via exosomes, A549 cells were grown in A549/anlotinib-CM and exosome-depleted A549/anlotinib-CM respectively. As shown in Figure 5A and 5B, A549 cells cultured in A549/anlotinib-CM expressed a higher level of miR-136-5p, whereas the level of miR-136-5p in A549 cells was decreased when exosomes from A549/anlotinib-CM were depleted. Next, A549 cells were indirectly co-cultured with A549/anlotinib cells that transiently transfected with Cy3-tagged miR-136-5p. As indicated in Figure 5C, Cy3 fluorescence dye was observed in A549 cells, suggesting that miR-136-5p is contained in A549/anlotinib cells-secreted exosomes and can be transferred to A549 cells. In addition, we further explored the existing pattern of extracellular miR-136-5p. RNase A treatment had very limited effect on miR-136-5p level in A549/anlotinib-CM; however, RNase A combined with Triton X-100 treatment markedly downregulated miR-136-5p level in A549/anlotinib-CM (Figure 5D), suggesting that extracellular miR-136-5p was largely encased within the membrane. Meanwhile, miR-136-5p levels were almost equal in whole A549/anlotinib-CM and A549/anlotinib-Exo (Figure 5E).

Additionally, the level of miR-136-5p was upregulated in A549/anlotinib cells transfected with miR-136-5p agomir (A549/anlotinib-miR-136-5p agomir), while miR-136-5p level was downregulated in A549/anlotinib cells transfected with miR-136-5p antagomir (A549/anlotinib-miR-136-5p antagomir) (Figure 5F). We then isolated exosomes from A549/anlotinib-miR-136-5p agomir-CM (A549/anlotinib-miR-136-5p agomir-Exo) and A549/anlotinib-miR-136-5p antagomir-CM (A549/anlotinib-miR-136-5p antagomir-Exo) respectively and confirmed their identity by the exosome surface markers TSG101 and CD91 (Figure 5G). Moreover, miR-136-5p level was increased in A549/anlotinib-miR-136-5p agomir-Exo; whereas miR-136-5p level was decreased in A549/anlotinib-miR-136-5p antagomir-Exo (Figure 5H). Functionally, A549 cells incubated with A549/anlotinib-miR-136-5p agomir-Exo displayed reduced sensitivity to anlotinib compared with A549/anlotinib-Exo group, while A549/anlotinib-miR-136-5p antagomir-Exo displayed the opposite results (Figure 5I). Collectively, A549/anlotinib cell-derived functional miR-136-5p could be delivered into A549 cells via exosomes.

MiR-136-5p promoted A549 cell proliferation and anlotinib resistance

Next, we investigated whether miR-136-5p could confer anlotinib resistance in NSCLC cells. MiR-136-5p agomir obviously increased the proliferation of A549 cells, while miR-136-5p antagomir markedly inhibited cell proliferation (Figure 6A). In addition, CCK-8, EdU staining assays showed that miR-136-5p agomir obviously promoted A549 cell proliferation and anlotinib resistance; however, miR-136-5p antagomir notably reduced A549 cell proliferation and anlotinib resistance (Figure 6B and 6C). Moreover, miR-136-5p agomir significantly inhibited anlotinib-induced apoptosis in A549 cells; whereas miR-136-5p antagomir displayed the opposite results (Figure 6D). Meanwhile, anlotinib notably induced cell cycle arrest at the G0-G1 phase in A549 cells (Figure 6E). However, miR-136-5p agomir significantly inhibited anlotinib-induced cell cycle arrest in A549 cells; whereas miR-136-5p antagomir displayed the opposite results (Figure 6E). Collectively, miR-136-5p could promote A549 cell proliferation and anlotinib resistance.

PPP2R2A is a direct target of exosomal miR-136-5p in NSCLC

The data in online bioinformatics tool TargetScan showed that PPP2R2A might be a potential target of miR-136-5p (Figure 7A). In addition, the luciferase activity of 3' UTR of PPP2R2A were suppressed by miR-136-5p agomir, suggesting that miR-136-5p could specifically bind to PPP2R2A (Figure 7B). Moreover, miR-136-5p agomir markedly downregulated the expression of PPP2R2A in A549 cells; whereas miR-136-5p antagomir displayed the opposite results (Figure 7C). As expected, A549/anlotinib-Exo notably decreased the expression of PPP2R2A in A549 cells (Figure 7C). These results indicated that PPP2R2A was a direct target of exosomal miR-136-5p in NSCLC.

MiR-136-5p promoted A549 cell proliferation and anlotinib resistance via downregulation of PPP2R2A

To investigate the functional role of PPP2R2A in miR-136-5p mediated anlotinib resistance in NSCLC cells, A549 cells were transfected with PPP2R2A siRNA1 and PPP2R2A siRNA2. As shown in Figure 7D, PPP2R2A siRNA2 remarkedly reduced the expression of PPP2R2A in A549 cells. Additionally, PPP2R2A siRNA2 decreased the expression of PPP2R2A and increased the expressions of p-Akt, Bcl-2 and XIAP in anlotinib-treated A549 cells (Figure 7E). Moreover, the results of CCK-8 assay showed that PPP2R2A siRNA2 markedly promoted A549 cell proliferation and anlotinib resistance (Figure 7F). Meanwhile, A549 cells transfected with miR-136-5p antagomir displayed increased sensitivity to anlotinib, which could be abolished by PPP2R2A siRNA2 (Figure 7G). Furthermore, miR-136-5p antagomir enhanced sensitivity of A549 cells to anlotinib via upregulation of PPP2R2A and downregulation of p-Akt, Bcl-2 and XIAP; whereas PPP2R2A downregulation in A549 cells abolished this effect (Figure 7H). To sum up, miR-136-5p could promote A549 cell proliferation and anlotinib resistance via downregulation of PPP2R2A.

A549/anlotinib cell-derived exosomal miR-136-5p agomir promoted A549 cell anlotinib resistance *in vivo*

To assess the effect of exosomal miR-136-5p on anlotinib response *in vivo*, we administered A549/anlotinib-Exo intratumorally into A549 xenografts. As shown in Figure 8A, 8B and 8C, A549/anlotinib-Exo or A549/anlotinib-miR-136-5p agomir-Exo remarkedly dampened the response of A549 xenografts to anlotinib, accompanied by upregulated miR-136-5p level in tumor tissues. In addition, A549/anlotinib-miR-136-5p agomir-Exo suppressed cell apoptosis in xenograft tumors upon anlotinib treatment; whereas A549/anlotinib-miR-136-5p antagomir-Exo displayed the opposite results (Figure 8D). Meanwhile, exosomal miR-136-5p notably decreased the expression of PPP2R2A and increased the expression of p-Akt in xenograft tumors upon anlotinib treatment; whereas A549/anlotinib-miR-136-5p antagomir-Exo displayed the opposite results (Figure 8E). These data indicated that A549/anlotinib cell-derived exosomal miR-136-5p promoted A549 cell anlotinib resistance *in vivo* via downregulation of PPP2R2A.

Discussion

The response of patients with advanced NSCLC to chemotherapy is poor, owing to intrinsic and acquired chemoresistance (22-24). At present, anlotinib is used for the third-line treatment of patients with

advanced NSCLC (25). However, acquired resistance to anlotinib has been observed in the clinic in patients with advanced NSCLC (25). Thus, it is necessary to investigate the molecular mechanisms underlying anlotinib resistance and identify potential targets for anlotinib-resistance therapy. In the present study, we found that miR-136-5p is highly expressed in anlotinib-resistant NSCLC. In addition, overexpression of miR-136-5p promoted anlotinib-resistance by targeting PPP2R2A, leading to the activation of Akt pathway. Moreover, miR-136-5p could be transferred from anlotinib-resistant NSCLC cells to anlotinib-sensitive NSCLC cells via exosomes, transforming anlotinib-sensitive cells into resistant cells, thereby disseminating anlotinib resistance.

Illuminating the molecular mechanisms of anlotinib resistance could contribute to the development of combination therapies to overcome anlotinib resistance. Evidences have shown that exosomes play an important role in chemoresistance in NSCLC (26). In addition, tumor-derived exosome can deliver various drug resistance-associated miRNAs to recipient cells (27). Thus, in this study, we performed RNA-sequencing assay to identify the DEMs in exosomes that isolated from plasma samples from patients with good anlotinib response and patients with poor anlotinib response. We found that miR-136-5p level was upregulated in exosomes-derived from plasma samples in patients who exhibited a poor response to anlotinib therapy. In addition, the level of miR-136-5p is increased in anlotinib-resistant NSCLC cells, as well as in the plasma of mice xenografted with A549/anlotinib cells. Therefore, exosomal miR-136-5p might be play an important role in anlotinib resistance.

It has been shown that secreted exosomes loaded with miRNAs could modulate cell biological function and cell signaling in recipient cells (28, 29). Fan et al showed that exosomal miR-210 derived from lung cancer cells could promote the fibroblasts transferring into cancer-associated fibroblasts (30). Kim et al found that NSCLC cell-derived exosomal miR-619-5p could promote tumor angiogenesis and metastasis by targeting RCAN1.4 (31). Importantly, exosomal miRNAs may play a vital role in mediating resistance transfer from tumor drug-resistant cells to tumor cells (32). In addition, the ability of exosomal miRNAs released by drug-resistant tumor cells to transfer the resistant phenotype to sensitive cells has been recognized as a key mechanism for dissemination of drug resistance (33). In this study, we found that miR-136-5p could be transferred from anlotinib-resistant NSCLC cells to anlotinib-sensitive NSCLC cells via exosomes. In addition, anlotinib-resistant NSCLC cell-derived exosomal miR-136-5p could confer the resistant phenotype to anlotinib-sensitive NSCLC cells. Furthermore, overexpression of miR-136-5p could promote the proliferation and suppress the apoptosis of anlotinib-sensitive NSCLC cells upon anlotinib treatment; whereas downregulation of miR-136-5p suppressed the proliferation and induced the apoptosis of anlotinib-sensitive NSCLC cells upon anlotinib treatment. Evidences have shown that upregulated miR-136 is associated with increased cell proliferation in human cancers, such as gastric cancer and NSCLC (34, 35), which were consistent with our data.

Next, we found that PPP2R2A were a binding target of miR-136-5p, which could be inversely regulated by miR-136-5p. PPP2R2A is considered as an tumor suppressor in human cancers (36, 37). Yu et el reported that overexpression of miR-221 could promote osteosarcoma cell proliferation and cisplatin resistance via downregulation of PPP2R2A (38). Shen et showed that miR-136-5p could promote the proliferation of

NSCLC cells via downregulation of PPP2R2A, which was consistent with our results (35). In this study, we found that downregulation of PPP2R2A could promote A549 cell proliferation and anlotinib resistance. Significantly, miR-136-5p could promote A549 cell proliferation and anlotinib resistance via downregulation of PPP2R2A. Collectively, exosomal miR-136-5p functionally promote cell proliferation and anlotinib resistance by targeting PPP2R2A after being delivered from anlotinib-resistant NSCLC cells to anlotinib-sensitive NSCLC cells.

Conclusion

In this study, we found that anlotinib-resistant NSCLC cell-derived exosomal miR-136-5p could promote NSCLC cell proliferation and anlotinib resistance by targeting PPP2R2A. Meanwhile, exosomal miR-136-5p antagomir from anlotinib-resistant NSCLC cells could functionally restore the anlotinib response in NSCLC cells. Therefore, miR-136-5p may act as a potential biomarker for anlotinib response in NSCLC.

Declarations

Ethics approval and consent to participate

All animal procedures were approved by the ethics committee of the Affiliated Lianyungang Hospital of Xuzhou Medical University.

Consent for publication

Not applicable.

Availability of data and materials

The datasets used and/or analyzed during the current study are available from the corresponding author on reasonable request.

Competing interests

The authors declare that they have no conflicts of interest.

Funding

1. Jiangsu Province Key Research and Development Plan (Social Development) Project (No. BE2017684).
2. Scientific Research Project of Jiangsu Health and Family Planning Commission (No. H2017039).
3. Natural Science Foundation of Jiangsu Province, China (No. BK20191211).

Authors' contributions

Guoqing Gu and Chenxi Hu made major contributions to the conception, design and manuscript drafting of this study. Kaiyuan Hui, Huiqin Zhang, Ting Chen and Xin Zhang were responsible for data acquisition, data analysis, data interpretation and manuscript revision. Xiaodong Jiang made substantial contributions to conception and design of the study and revised the manuscript critically for important intellectual content. All authors agreed to be accountable for all aspects of the work. All authors read and approved the final manuscript.

Acknowledgements

Not applicable.

References

1. Bai Y, Liu X, Qi X, Liu X, Peng F, Li H, et al. PDIA6 modulates apoptosis and autophagy of non-small cell lung cancer cells via the MAP4K1/JNK signaling pathway. EBioMedicine. 2019;42:311–25.
2. Feng H, Ge F, Du L, Zhang Z, Liu D. MiR-34b-3p represses cell proliferation, cell cycle progression and cell apoptosis in non-small-cell lung cancer (NSCLC) by targeting CDK4. J Cell Mol Med. 2019;23(8):5282–91.
3. Ridge CA, McErlean AM, Ginsberg MS. Epidemiology of lung cancer. Semin Interv Radiol. 2013;30(2):93–8.
4. Liu X, Zhong D. [Research Progress of Immune Checkpoint Inhibitor Therapy for BRAF Mutation in Non-small Cell Lung Cancer]. Zhongguo fei ai za zhi = Chinese. journal of lung cancer. 2019;22(9):583–9.
5. Herbst RS, Heymach JV, Lippman SM. Lung cancer. N Engl J Med. 2008;359(13):1367–80.
6. Liang L, Hui K, Hu C, Wen Y, Yang S, Zhu P, et al. Autophagy inhibition potentiates the anti-angiogenic property of multikinase inhibitor anlotinib through JAK2/STAT3/VEGFA signaling in non-small cell lung cancer cells. Journal of experimental clinical cancer research: CR. 2019;38(1):71.
7. Han B, Li K, Wang Q, Zhang L, Shi J, Wang Z, et al. Effect of Anlotinib as a Third-Line or Further Treatment on Overall Survival of Patients With Advanced Non-Small Cell Lung Cancer: The ALTER 0303 Phase 3 Randomized Clinical Trial. JAMA oncology. 2018;4(11):1569–75.
8. Théry C. Exosomes: secreted vesicles and intercellular communications. F1000 biology reports. 2011;3:15.
9. Zhang L, Yu D. Exosomes in cancer development, metastasis, and immunity. Biochimica et biophysica acta Reviews on cancer. 2019;1871(2):455–68.
10. Yu X, Odenthal M, Fries JW. Exosomes as miRNA Carriers: Formation-Function-Future. International journal of molecular sciences. 2016;17(12).
11. Li S, Li Y, Chen B, Zhao J, Yu S, Tang Y, et al. exoRBase: a database of circRNA, lncRNA and mRNA in human blood exosomes. Nucleic acids research. 2018;46(D1):D106-d12.

12. Raposo G, Stoorvogel W. Extracellular vesicles: exosomes, microvesicles, and friends. J Cell Biol. 2013;200(4):373–83.
13. Ganju A, Khan S, Hafeez BB, Behrman SW, Yallapu MM, Chauhan SC, et al. miRNA nanotherapeutics for cancer. Drug discovery today. 2017;22(2):424–32.
14. Ji Q, Xu X, Song Q, Xu Y, Tai Y, Goodman SB, et al. miR-223-3p Inhibits Human Osteosarcoma Metastasis and Progression by Directly Targeting CDH6. Molecular therapy: the journal of the American Society of Gene Therapy. 2018;26(5):1299–312.
15. Bushati N, Cohen SM. microRNA functions. Annual review of cell and developmental biology. 2007;23:175–205.
16. Jayaraj R, Nayagam SG, Kar A, Sathyakumar S, Mohammed H, Smiti M, et al. Clinical Theragnostic Relationship between Drug-Resistance Specific miRNA Expressions, Chemotherapeutic Resistance, and Sensitivity in Breast Cancer: A Systematic Review and Meta-Analysis. Cells. 2019;8(10).
17. Wu J, Mao X, Cai T, Luo J, Wei L. KOBAS server: a web-based platform for automated annotation and pathway identification. Nucleic acids research. 2006;34(Web Server issue):W720-4.
18. Zhang J, Li S, Li L, Li M, Guo C, Yao J, et al. Exosome and exosomal microRNA: trafficking, sorting, and function. Genom Proteom Bioinform. 2015;13(1):17–24.
19. Wang X, Xu J, Chen J, Jin S, Yao J, Yu T, et al. IL-22 Confers EGFR-TKI Resistance in NSCLC via the AKT and ERK Signaling Pathways. Frontiers in oncology. 2019;9:1167.
20. Sun CY, Zhu Y, Li XF, Wang XQ, Tang LP, Su ZQ, et al. Scutellarin Increases Cisplatin-Induced Apoptosis and Autophagy to Overcome Cisplatin Resistance in Non-small Cell Lung Cancer via ERK/p53 and c-met/AKT Signaling Pathways. Front Pharmacol. 2018;9:92.
21. Zhang W, Song C, Ren X. Circ_0003998 Regulates the Progression and Docetaxel Sensitivity of DTX-Resistant Non-Small Cell Lung Cancer Cells by the miR-136-5p/CORO1C Axis. Technology in cancer research treatment. 2021;20:1533033821990040.
22. Grootjans W, de Geus-Oei LF, Troost EG, Visser EP, Oyen WJ, Bussink J. PET in the management of locally advanced and metastatic NSCLC. Nature reviews Clinical oncology. 2015;12(7):395–407.
23. Doval DC, Desai CJ, Sahoo TP. Molecularly targeted therapies in non-small cell lung cancer: The evolving role of tyrosine kinase inhibitors. Indian journal of cancer. 2019;56(Supplement):23-s30.
24. Wang Y, Wen L, Zhao SH, Ai ZH, Guo JZ, Liu WC. FoxM1 expression is significantly associated with cisplatin-based chemotherapy resistance and poor prognosis in advanced non-small cell lung cancer patients. Lung cancer (Amsterdam Netherlands). 2013;79(2):173–9.
25. Han B, Li K, Zhao Y, Li B, Cheng Y, Zhou J, et al. Anlotinib as a third-line therapy in patients with refractory advanced non-small-cell lung cancer: a multicentre, randomised phase II trial (ALTER0302). British journal of cancer. 2018;118(5):654–61.
26. Lobb RJ, van Amerongen R, Wiegmans A, Ham S, Larsen JE, Möller A. Exosomes derived from mesenchymal non-small cell lung cancer cells promote chemoresistance. International journal of cancer. 2017;141(3):614–20.

27. Santos JC, Lima NDS, Sarian LO, Matheu A, Ribeiro ML, Derchain SFM. Exosome-mediated breast cancer chemoresistance via miR-155 transfer. Scientific reports. 2018;8(1):829.
28. Zhang C, Zhang K, Huang F, Feng W, Chen J, Zhang H, et al. Exosomes, the message transporters in vascular calcification. J Cell Mol Med. 2018;22(9):4024–33.
29. Melo SA, Sugimoto H, O'Connell JT, Kato N, Villanueva A, Vidal A, et al. Cancer exosomes perform cell-independent microRNA biogenesis and promote tumorigenesis. Cancer cell. 2014;26(5):707–21.
30. Fan J, Xu G, Chang Z, Zhu L, Yao J. miR-210 transferred by lung cancer cell-derived exosomes may act as proangiogenic factor in cancer-associated fibroblasts by modulating JAK2/STAT3 pathway. Clinical science (London, England: 1979). 2020;134(7):807 – 25.
31. Kim DH, Park S, Kim H, Choi YJ, Kim SY, Sung KJ, et al. Tumor-derived exosomal miR-619-5p promotes tumor angiogenesis and metastasis through the inhibition of RCAN1.4. Cancer letters. 2020;475:2–13.
32. Yang Z, Zhao N, Cui J, Wu H, Xiong J, Peng T. Exosomes derived from cancer stem cells of gemcitabine-resistant pancreatic cancer cells enhance drug resistance by delivering miR-210. Cellular oncology (Dordrecht). 2020;43(1):123–36.
33. Sousa D, Lima RT, Vasconcelos MH. Intercellular Transfer of Cancer Drug Resistance Traits by Extracellular Vesicles. Trends Mol Med. 2015;21(10):595–608.
34. Chen X, Huang Z, Chen R. Microrna-136 promotes proliferation and invasion ingastric cancer cells through Pten/Akt/P-Akt signaling pathway. Oncology letters. 2018;15(4):4683–9.
35. Shen S, Yue H, Li Y, Qin J, Li K, Liu Y, et al. Upregulation of miR-136 in human non-small cell lung cancer cells promotes Erk1/2 activation by targeting PPP2R2A. Tumour biology: the journal of the International Society for Oncodevelopmental Biology Medicine. 2014;35(1):631–40.
36. Qiu Z, Fa P, Liu T, Prasad CB, Ma S, Hong Z, et al. A Genome-Wide Pooled shRNA Screen Identifies PPP2R2A as a Predictive Biomarker for the Response to ATR and CHK1 Inhibitors. Cancer research. 2020;80(16):3305–18.
37. Li R, Li J, Yang H, Bai Y, Hu C, Wu H, et al. Hepsin Promotes Epithelial-Mesenchymal Transition and Cell Invasion Through the miR-222/PPP2R2A/AKT Axis in Prostate Cancer. OncoTargets therapy. 2020;13:12141–9.
38. Yu WC, Chen HH, Qu YY, Xu CW, Yang C, Liu Y. MicroRNA-221 promotes cisplatin resistance in osteosarcoma cells by targeting PPP2R2A. Bioscience reports. 2019;39(7).

Tables

Table 1 Clinical characteristics of NSCLC patients in anlotinib treatment.

	NSCLC patients (n=15)
Age	
average	62.6
range	41-80
Gender	
male	8 (53.3%)
female	7 (46.7%)
Histologic type	
lung adenocarcinoma	14 (93.3%)
squamous cell lung carcinoma	1 (6.7%)
Furman grade	
III	0 (0%)
IV	15 (100%)
Treatment method before oral treatment with anlotinib	
radiotherapy	4 (26.7%)
chemotherapy	10 (66.7%)
antiangiogenic therapy	2 (13.3%)
surgery	4 (26.7%)
tumor targeted therapy	9 (60.0%)

Figures

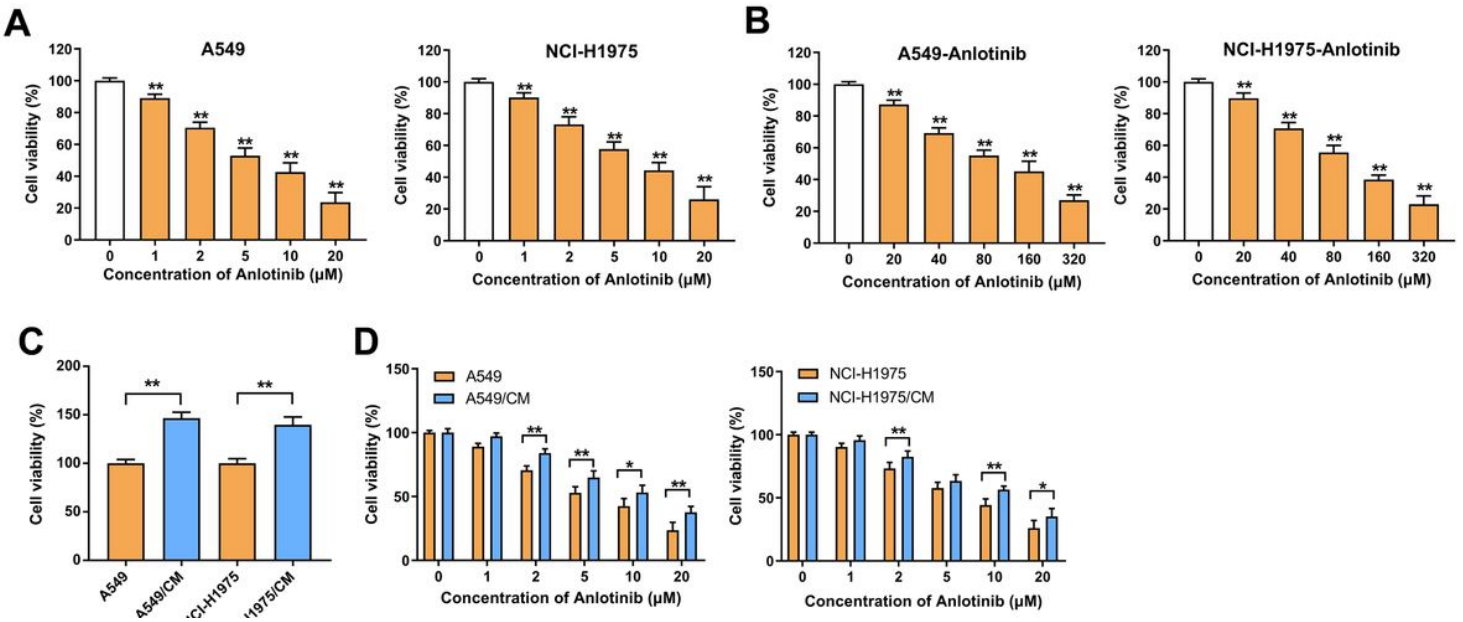

Figure 1

NSCLC/anlotinib cell increased NSCLC cell proliferation and anlotinib resistance. (A) CCK-8 assay of A549 or NCI-H1975 cells treated with anlotinib (0, 1, 2, 5, 10 or 20 μM) for 72 h. **P<0.01 compared with 0 μM group. (B) CCK-8 assay of A549/anlotinib or NCI-H1975/anlotinib cells treated with anlotinib (0, 20, 40, 80, 160 or 320 μM) for 72 h. **P<0.01 compared with 0 μM group. A549 cells were incubated in A549-CM or A549/anlotinib-CM for 3 days, NCI-H1975 cells were incubated in NCI-H1975-CM or NCI-H1975/anlotinib-CM for 3 days, (C) CCK-8 assay was used to determine the viability of A549 and NCI-H1975 cells; (D) CCK-8 assays were performed to determine the anlotinib response of these cells. *P<0.05, **P<0.01.

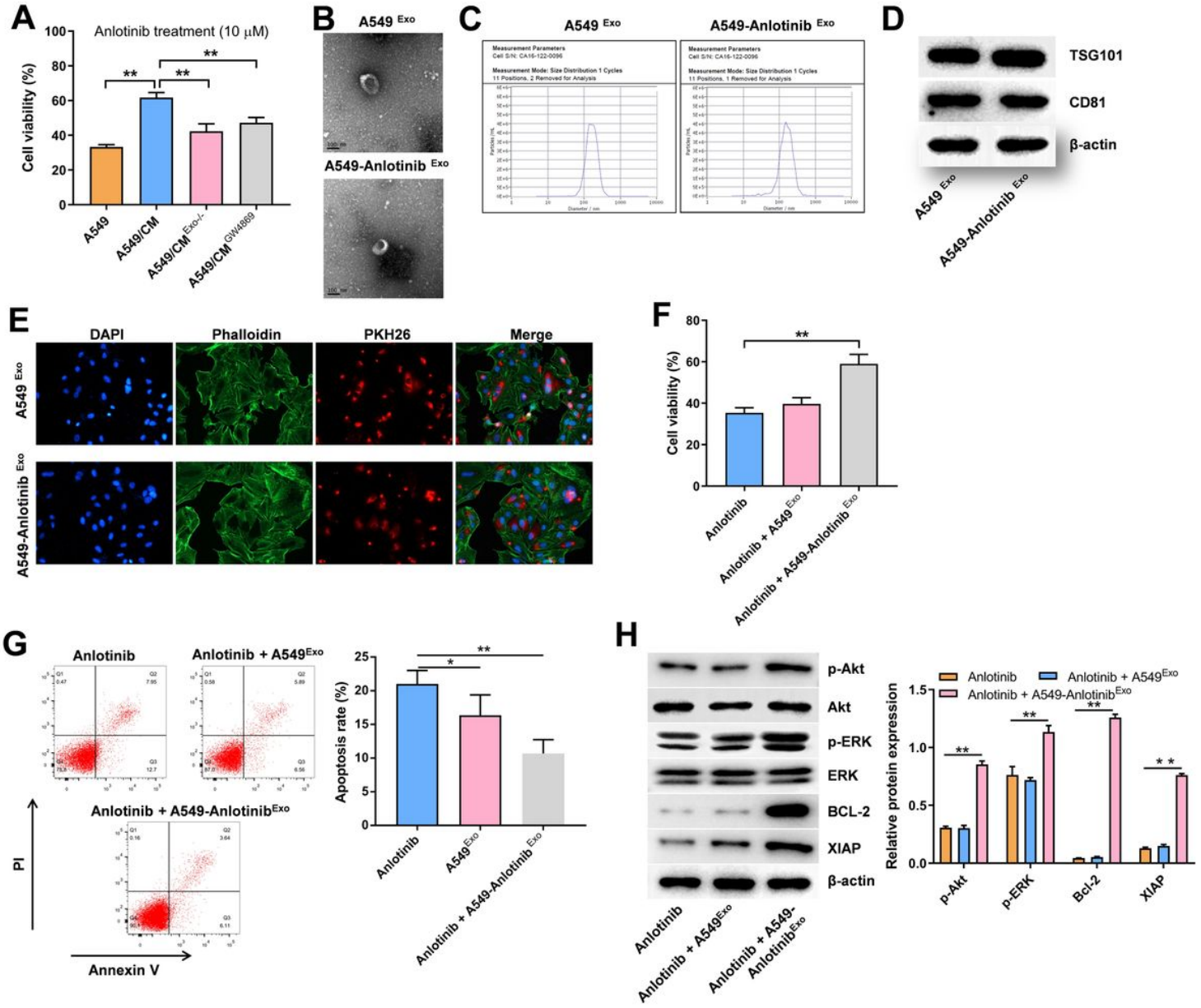

Figure 2

NSCLC/anlotinib cell-derived exosomes increased NSCLC cell proliferation and anlotinib resistance. (A) A549 cells were incubated in control-CM, A549/anlotinib-CM, exosome-depleted A549/anlotinib-CM, and A549 cells were co-cultured with GW4869-treated A549/anlotinib cells for 3 days. Cell viability was determined by CCK-8 assay upon anlotinib treatment. **P<0.01. (B, C, D) Identification of exosomes derived from A549 and A549/anlotinib cells by TEM, NTA and western blot analysis. (E) Fluorescent observation of A549 cells after incubation with PKH26-labeled exosomes from A549 or A549/anlotinib cells for 24 h. (F) A549 cells were incubated with exosomes from A549 (A549Exo) or A549/anlotinib cells (A549/anlotinibExo) for 48h, followed by anlotinib treatment for 72 h. Cell viability was measured by CCK-8 assay. **P<0.01. (G) Cell apoptosis was measured by flow cytometry assay. **P<0.01. (H) Western blot analysis of p-Akt, Akt, p-ERK, ERK, Bcl-2, XIAP in A549 cells. **P<0.01.

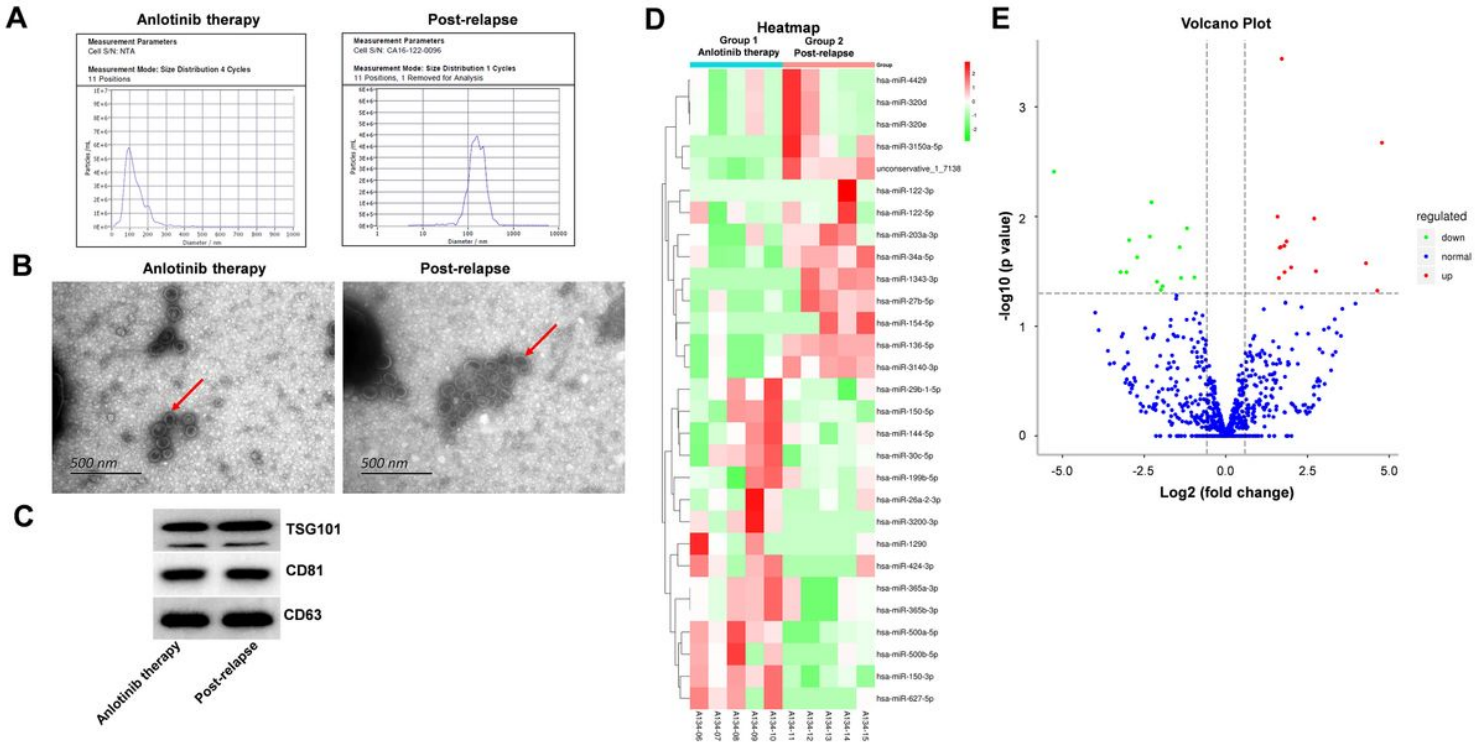

Figure 3

Identification of DEMs. (A, B, C) Exosomes were isolated from plasma samples in patients who exhibited a good response to anlotinib therapy and patients who exhibited a positive response to anlotinib initially and developed a resistance to anlotinib eventually. Exosomes were identified by TEM, NTA and western blot analysis. (D, E) Heat Map and Volcano plot showing the mRNA expression profiles of exosomes that isolated from plasma samples from patients who exhibited a good response to anlotinib therapy and patients who exhibited a positive response to anlotinib initially and developed a resistance to anlotinib eventually.

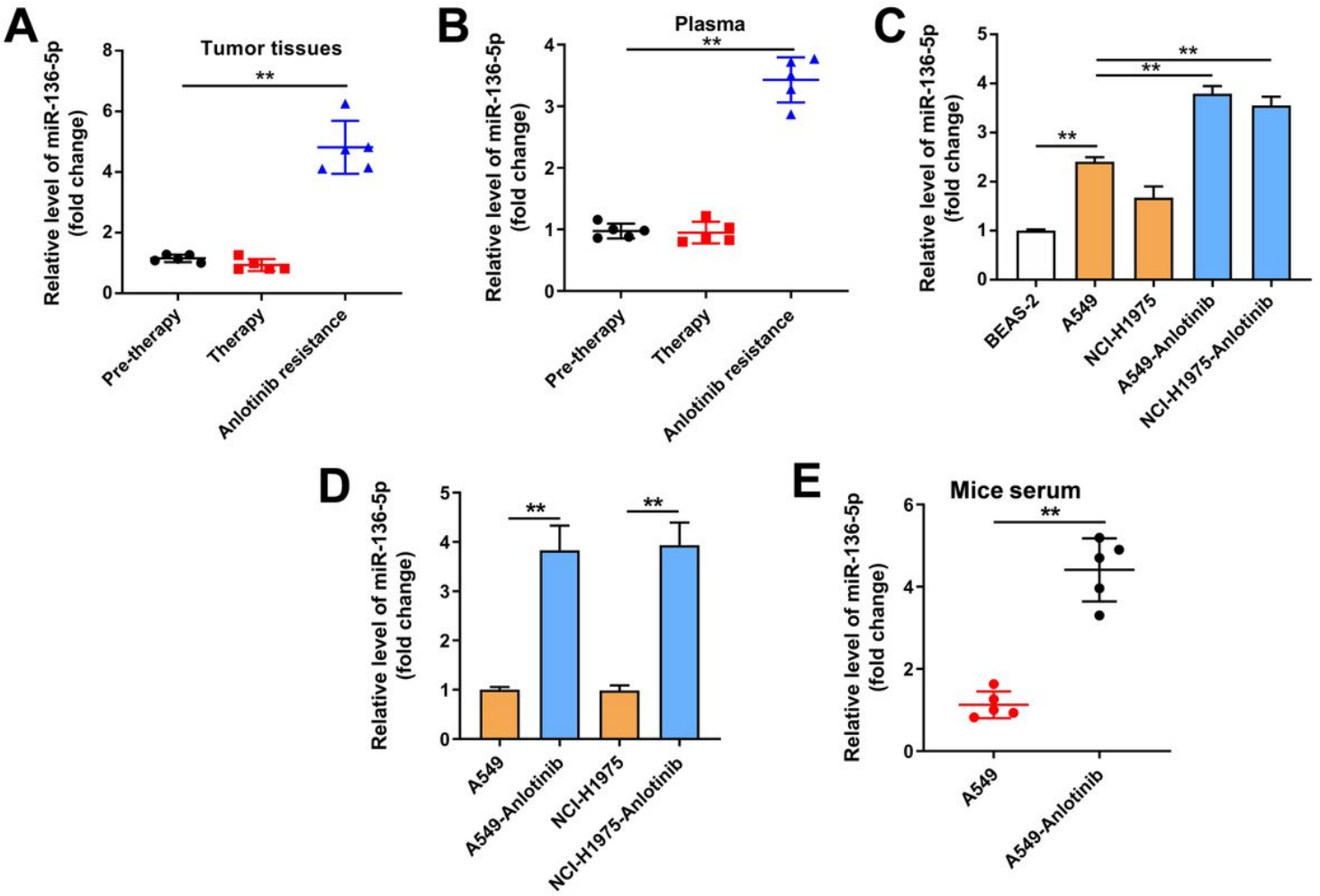

Figure 4

MiR-136-5p is highly expressed in anlotinib-resistant NSCLC cells. (A, B) RT-qPCR analysis of miR-136-5p level in tumor tissues and plasma from patients who exhibited a poor response to anlotinib therapy and patients who were therapy naïve or patients who exhibited a positive response to anlotinib therapy. (C) RT-qPCR analysis of miR-136-5p level in BEAS-2, A549, A549/anlotinib, NCI-H1975 and A549/anlotinib cells. (D) RT-qPCR analysis of miR-136-5p level in the CM of anlotinib-resistant and parental cells. (E) RT-qPCR analysis of miR-136-5p level in the serum of mice xenografted with anlotinib-resistant and parental A549 cells. **P<0.01.

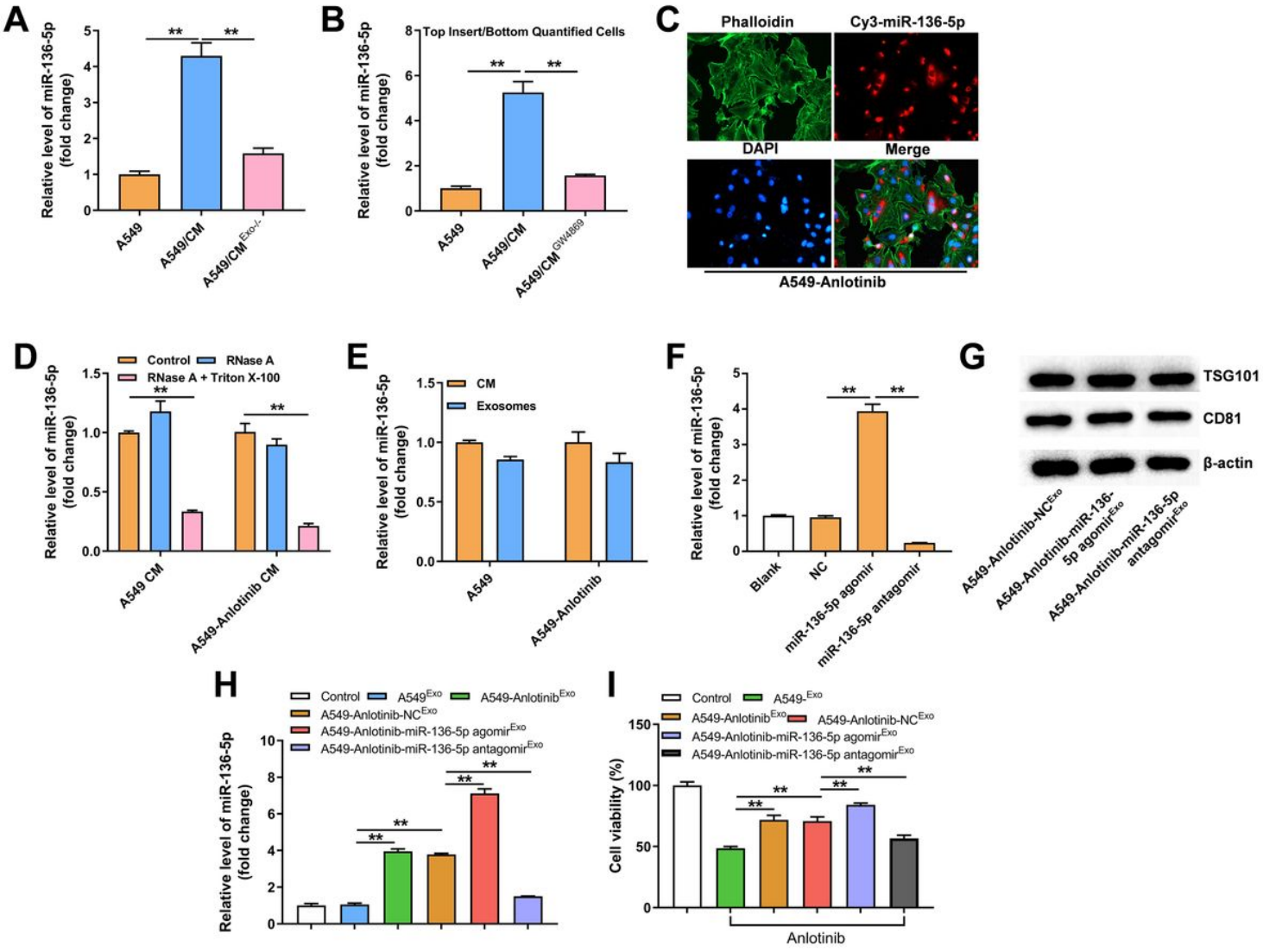

Figure 5

Exosomal transfer of miR-136-5p from anlotinib-resistant NSCLC cells to NSCLC cells. (A) RT-qPCR analysis of miR-136-5p level in A549 cells incubated with control-CM, A549/anlotinib-CM, exosome-depleted A549/anlotinib-CM. (B) RT-qPCR analysis of miR-136-5p level in A549 cells co-cultured with A549, A549/anlotinib and GW4869-treated A549/anlotinib cells. (C) A549/anlotinib cells transfected with Cy3-tagged miR-136-5p were co-cultured with A549 cells for 48 h, and the fluorescence signal was detected by microscopy. (D) RT-qPCR analysis of miR-136-5p level in the CM of A549 and A549/anlotinib cells treated with RNase A (2 mg/ml) alone or combined with Triton X-100 (0.1%) for 20 min. (E) RT-qPCR analysis of miR-136-5p level in A549-CM and A549/anlotinib cell-CM, A549-Exo and A549/anlotinib-Exo. (F) RT-qPCR analysis of miR-136-5p level in A549/anlotinib cells transfected with NC, miR-136-5p agomir and miR-136-5p antagomir. (G) Identification of exosomes derived from transfected A549/anlotinib cells by western blot analysis. (H) RT-qPCR analysis of miR-136-5p level in A549 cells after incubation with indicated exosomes. (I) CCK-8 assay of A549 cells pre-incubated with indicated exosomes for 48 h, followed by anlotinib treatment for 72 h. **P<0.01.

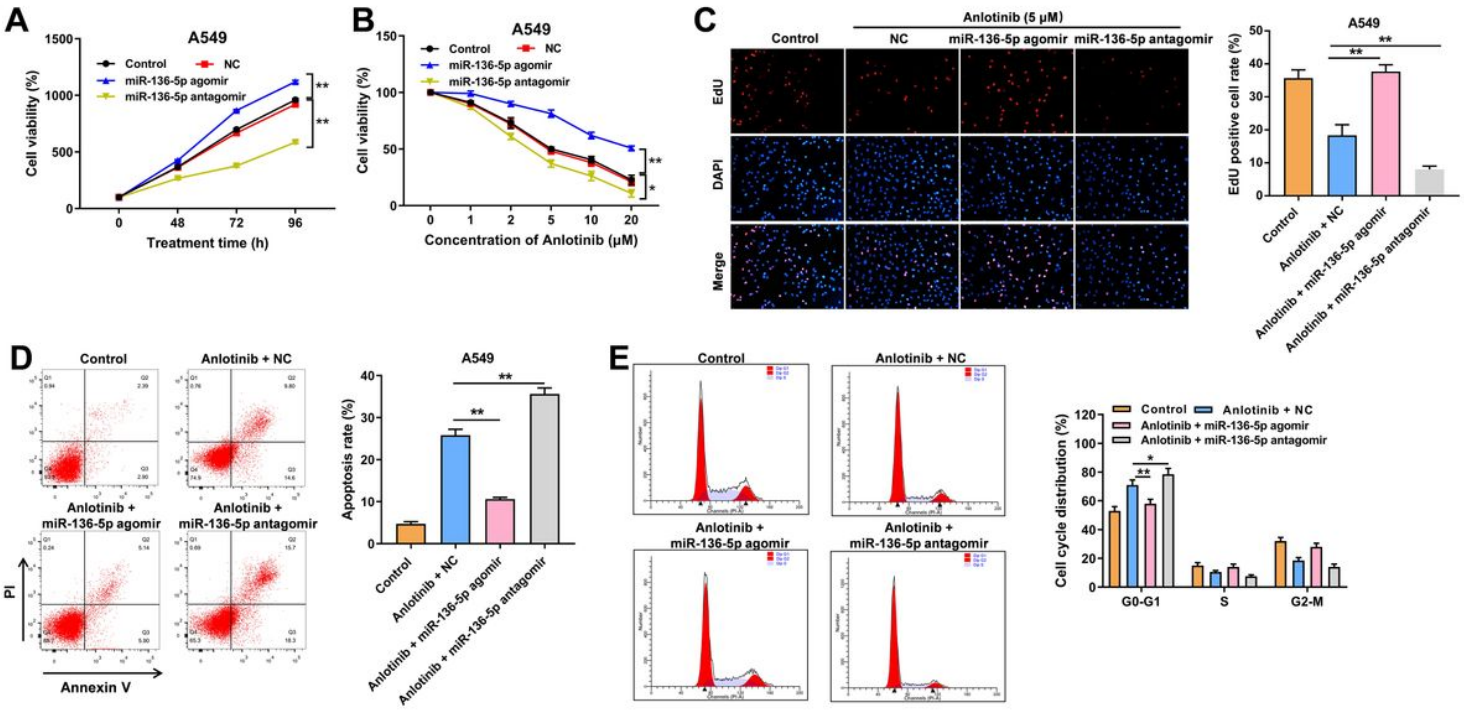

Figure 6

MiR-136-5p promoted A549 cell proliferation and anlotinib resistance. (A) CCK-8 assay of A549 cells treated with miR-136-5p agomir or miR-136-5p antagomir for 0, 48, 72 and 96 h. (B) A549 cells were treated with miR-136-5p agomir and antagomir for 48 h, followed by anlotinib treatment for 72 h. CCK-8 assay was used to assess cell viability. (C) EdU staining assay was used to assess cell proliferation. (D, E) Cell apoptosis and cell cycle distribution were determined by flow cytometry assay. *P<0.05, **P<0.01.

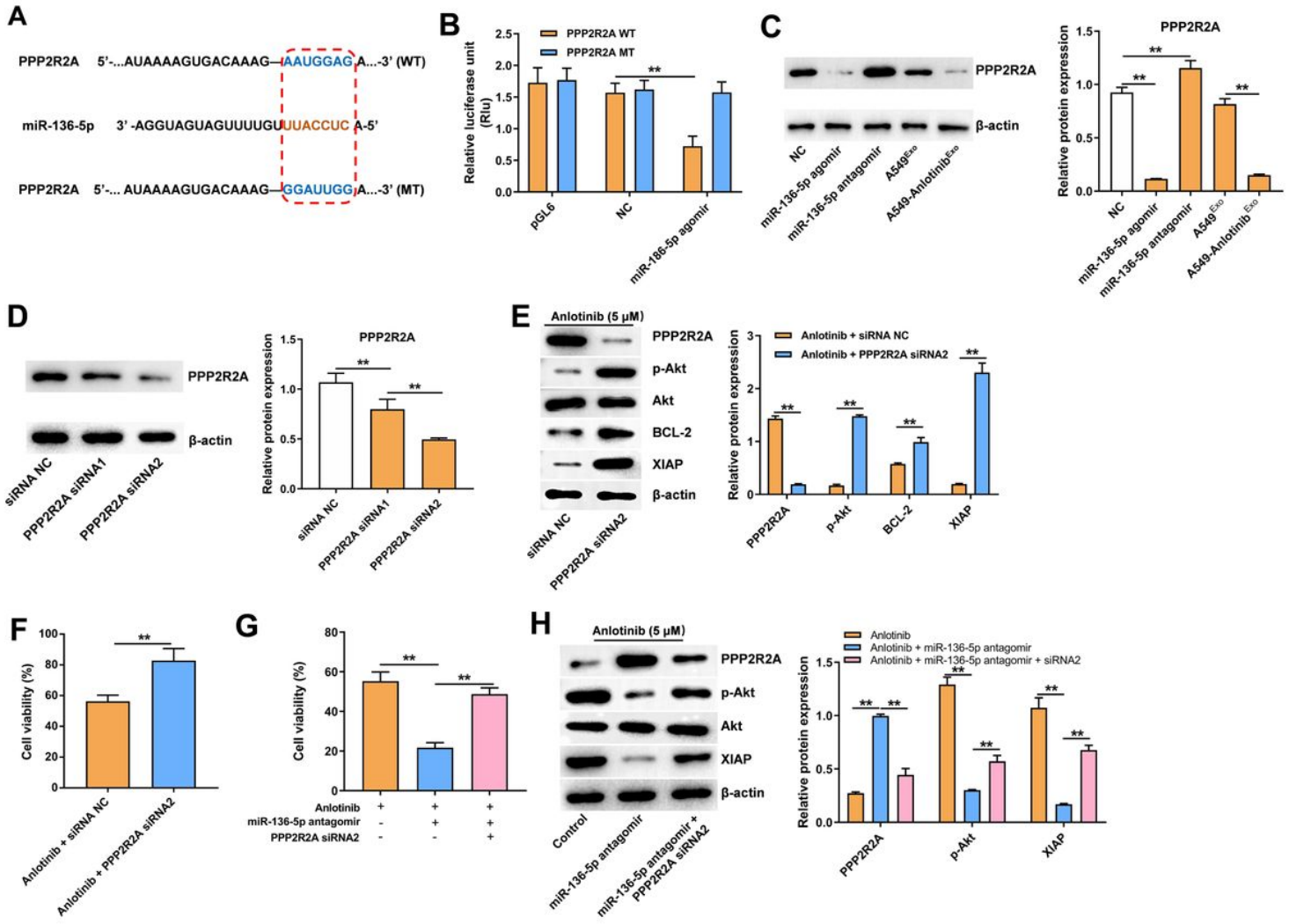

Figure 7

MiR-136-5p promoted A549 cell proliferation and anlotinib resistance via downregulation of PPP2R2A. (A) Schematic diagram of binding sites between miR-136-5p and PPP2R2A. (B) Luciferase reporter assay validated the relationship between miR-136-5p and PPP2R2A. (C) Western blot analysis of PPP2R2A expression in A549 cells treated with miR-136-5p agomir, miR-136-5p antagomir, A549-Exo and A549/anlotinib-Exo. (D) Western blot analysis of PPP2R2A expression in A549 cells transfected with PPP2R2A siRNA1 and siRNA2. (E) Western blot analysis of PPP2R2A, p-Akt, Akt, Bcl-2 and XIAP expressions in A549 cells transfected with PPP2R2A siRNA2, followed by anlotinib treatment. (F) CCK-8 assay of A549 cells transfected with PPP2R2A siRNA2, followed by anlotinib treatment. (G) Western blot analysis of PPP2R2A, p-Akt, Akt, Bcl-2 and XIAP expressions in A549 cells transfected with miR-136-5p antagomir or miR-136-5p antagomir plus PPP2R2A siRNA2, followed by anlotinib treatment. (H) CCK-8 assay of A549 cells transfected with miR-136-5p antagomir or miR-136-5p antagomir plus PPP2R2A siRNA2, followed by anlotinib treatment. **P<0.01.

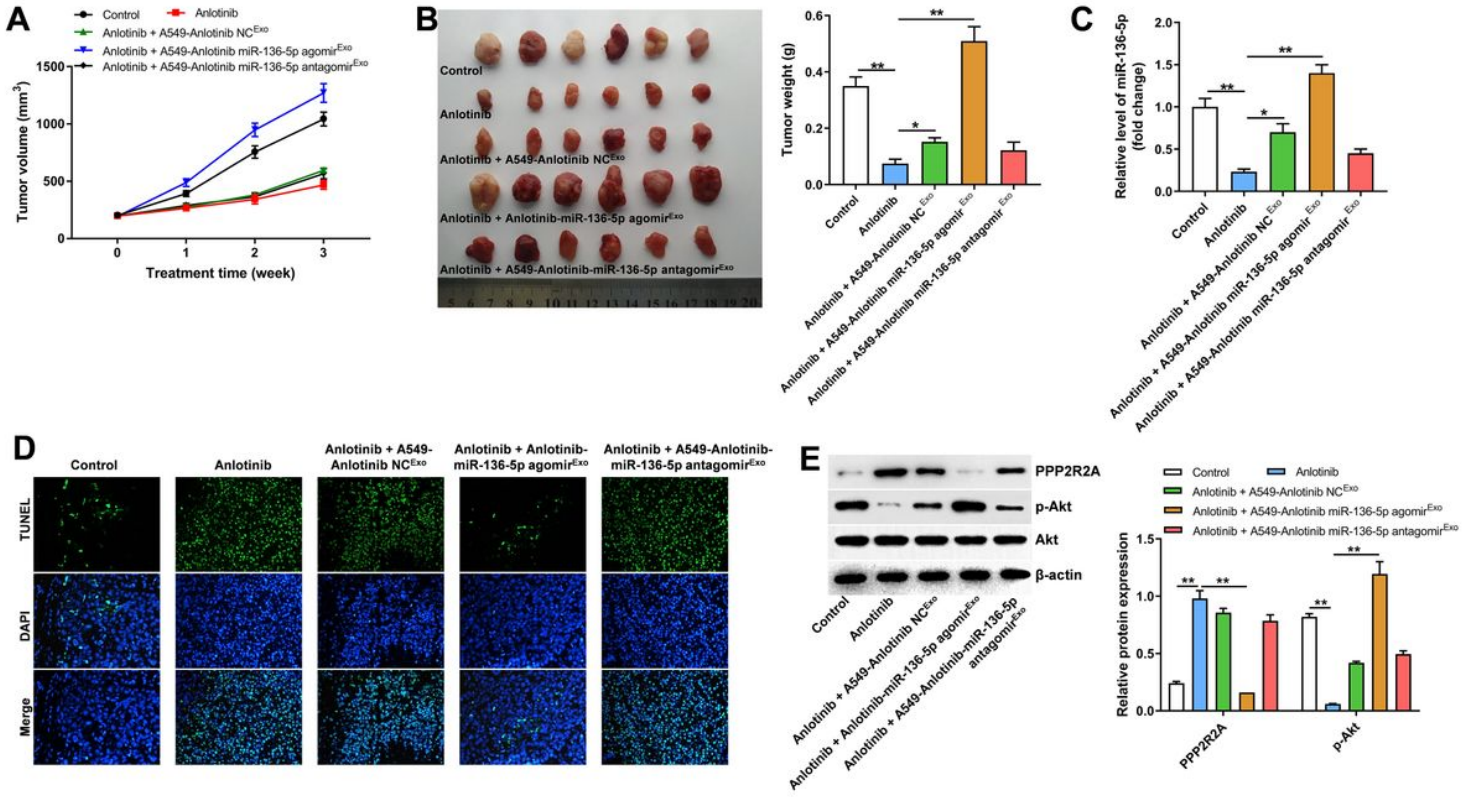

Figure 8

A549/anlotinib cell-derived exosomal miR-136-5p promoted A549 cell anlotinib resistance in vivo. (A) Tumor volume was measured. (B) Representative image of xenograft tumors and tumor weights. (C) RT-qPCR analysis of miR-136-5p level in tumor tissues. (D) Cell apoptosis in tumor tissues was assess using TUNEL assay. (E) Western blot analysis of PPP2R2A, p-Akt, Akt expressions in tumor tissues.

Supplementary Files

This is a list of supplementary files associated with this preprint. Click to download.

- Supplementaryfigure1.jpg
- Supplementaryfigure2.jpg